

## Supplementary information of

# Synthesis and crystal structures of a novel layered silicate SSA-1 and its microporous derivatives by topotactic transformation

*S. Takahashi,<sup>a</sup> Y. Kurita,<sup>a</sup> T. Ikeda,<sup>\*,b</sup> M. Miyamoto,<sup>c</sup> S. Uemiya,<sup>c</sup> and Y. Oumi<sup>\*,d</sup>*

<sup>a</sup>Graduate School of Engineering, Gifu University, Yanagido 1-1, Gifu, 501-1193, Japan.

<sup>b</sup>National Institute of Advanced industrial and Technology (AIST) Tohoku, 4-2-1, Nigatake, Miyagino-ku, Sendai, 983-8551, Japan.

<sup>c</sup>Faculty of Engineering, Gifu University, Yanagido 1-1, Gifu, 501-1193, Japan.

<sup>d</sup>Life Science Research Center, Gifu University, Yanagido 1-1, Gifu, 501-1193, Japan.

\* corresponding author

CORRESPONDING AUTHOR FOOTNOTE: Yasunori Oumi and Takuji Ikeda,

TEL: +81-58-293-2037, FAX: +81-58-293-2036 (oumi)

TEL: +81-22-237-3013, FAX: +81-22-237-5224 (ikeda)

E-mail: [oumi@gifu-u.ac.jp](mailto:oumi@gifu-u.ac.jp) and [takuji-ikeda@aist.go.jp](mailto:takuji-ikeda@aist.go.jp)

## 1. TG/DTA analysis of SSA-1

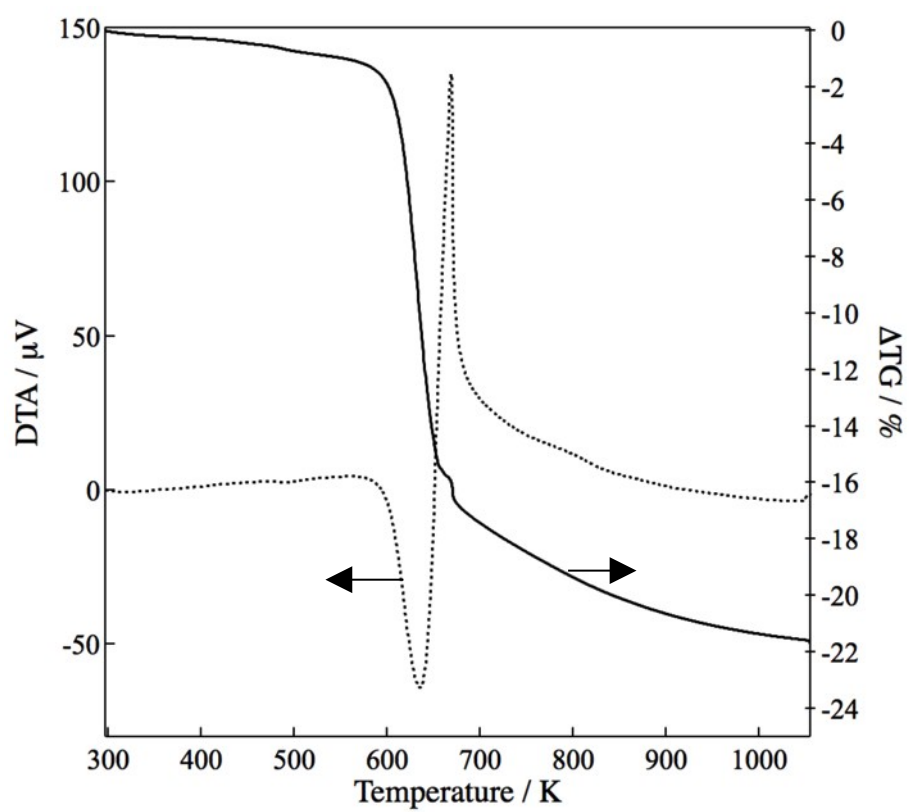


**Figure S1.** TG/DTA curves of SSA-1

## 2. Nitrogen gas adsorption measurements for PML-1 and IEZ-SSA-1

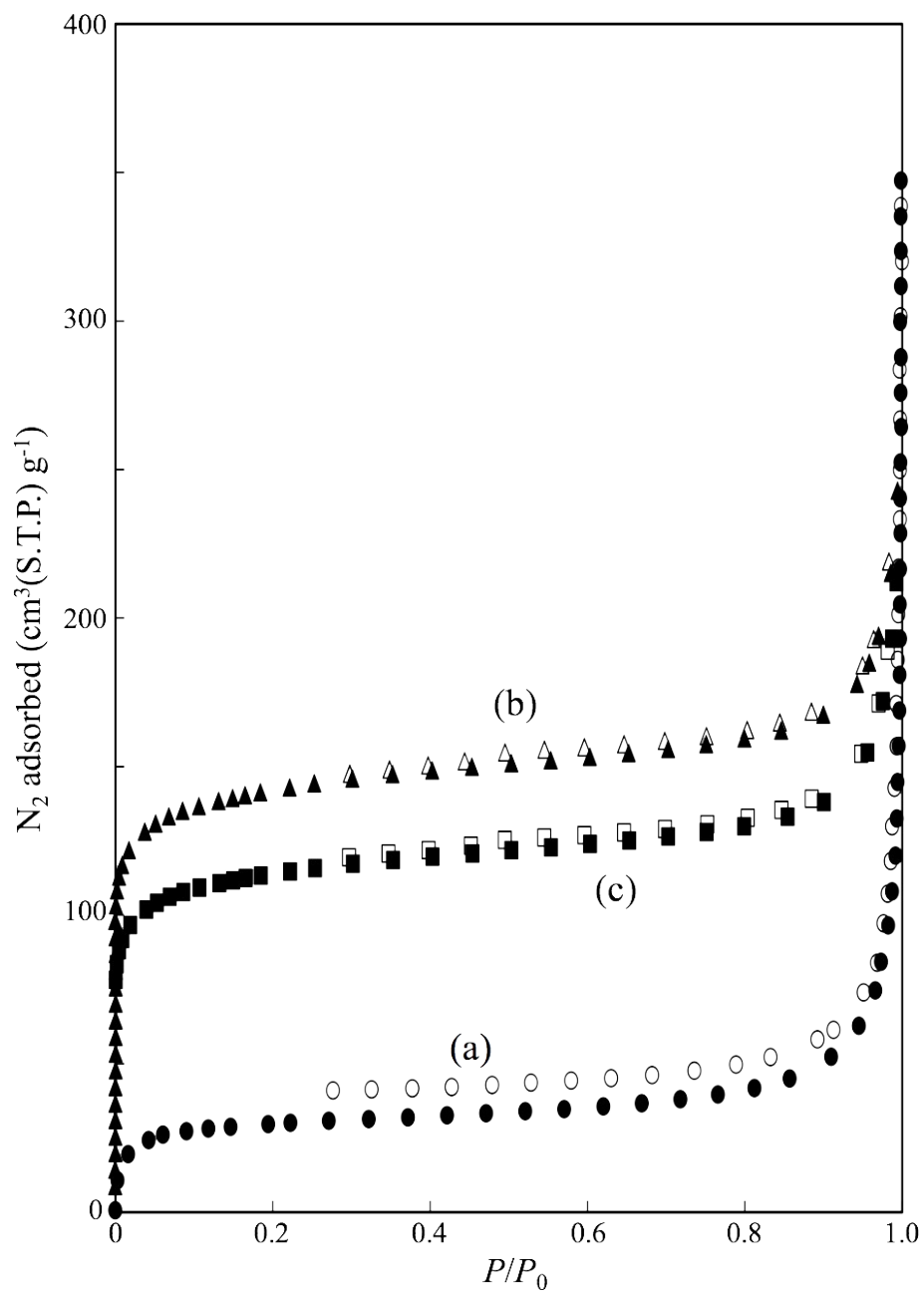


**Figure S2.** N<sub>2</sub> adsorption isotherm plots of (a) PML-1, (b) IEZ-SSA-1 (573 K) and (c) IEZ-SSA-1 (773 K). Fill mark and open mark indicate adsorption and desorption data, respectively, for each isotherm.

### 3. Crystal structure analysis of SSA-1

High resolution powder XRD data of SSA-1 and PML-1 were collected at room temperature on a Bruker D8 Advance with Vario-1 diffractometer (Bruker AXS, Ltd., Japan) in modified Debye-Scherrer geometry. The sample was packed into a borosilicate glass capillary with an inner diameter of 0.5 mm. This diffractometer equipped with a wide range position-sensitive detector (VANTEC-1) and a Ge(111) primary monochromator yielding  $\text{CuK}\alpha_1$  radiation.

Lattice constants were analyzed by indexing method using the program *N-Treor* built in EXPO2014. Reflection conditions derived from indices of reflections observed were  $l = 2m$  for  $hhl$  and  $l = 2m$  for  $00l$ , which gives a possible space groups:  $P2_1$  (No. 4, setting 1). This finding suggests that the layered framework structure of SSA-1 is identical with similar to that of HUS-2, although however stacking sequence of adjacent layers is largely different between them. Namely, lattice constants  $a$ ,  $c$  and  $\beta$  are very close to that of HUS-2. Lattice constant  $b$  is smaller than that of HUS-2, indicating that two silicate layers are stacked along  $b$ -axis and approach each other.

Observed structure factors,  $|F_{\text{obs}}|^2$ , of 1210 reflections in the region  $d > 1.07 \text{ \AA}$  were extracted by the Le Bail method. A framework structure was determined by the direct method using EXPO2014. At this stage, a few atoms, which would be attributed to a  $\text{TEA}^+$  cation, were found in an interlayer. However, they did not clarify by the direct method in detail. Distribution and conformation of  $\text{TEA}^+$  cation in the interlayer was investigated by the direct space method based on the parallel-tempering algorithm by means of the program FOX. In this analysis, the molecular structure of the  $\text{TEA}^+$  cation including proton was introduced into a structural model as a single atomic group with bond lengths and angles restrained within appropriate regions. Meanwhile, Si and O atom positions, which were found by the direct method analysis, were fixed at refined positions obtained by a preliminary Rietveld analysis. Then, optimized conformation of  $\text{TEA}^+$  or other guest molecules were introduced into the structure method. Several iterative analyses between Rietveld analysis and PT optimization took place until  $R_{\text{wp}}$  value decreased to  $< 10 \%$ . In this way, an initial structure model was constructed. Structure refinement was carried out with the aid of the Rietveld method using the program RIETAN-FP.

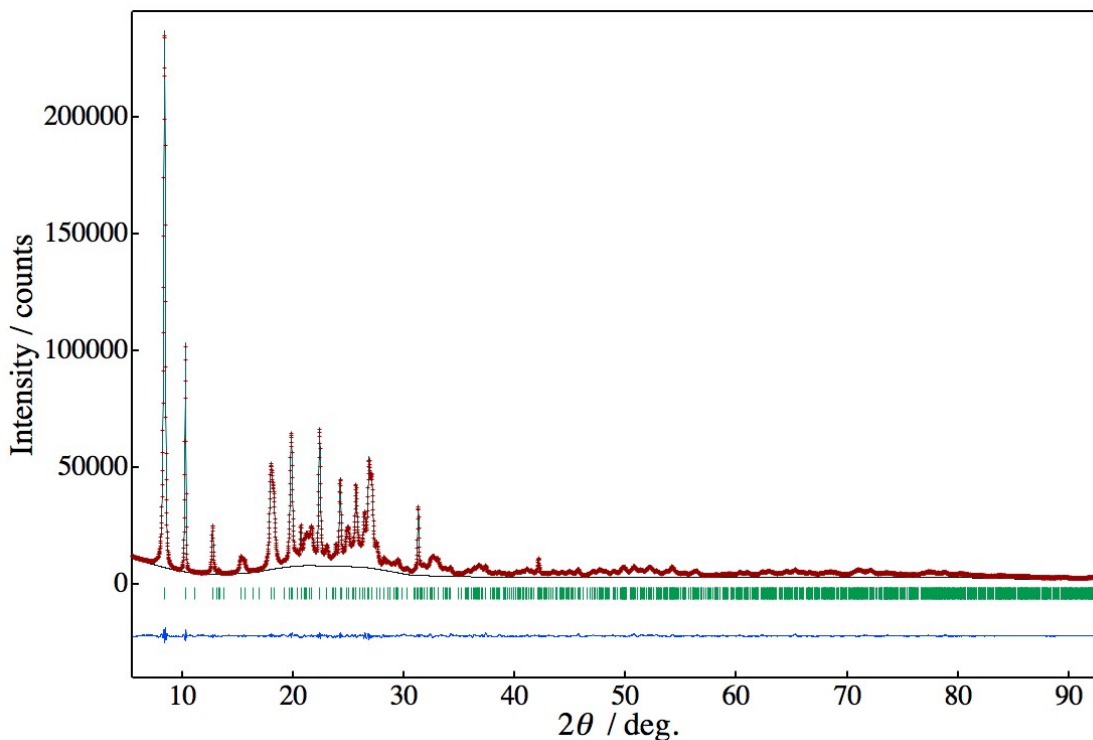


**Figure S3.** Observed pattern (red crosses), calculated pattern (light blue solid line), and difference pattern (blue) obtained by Rietveld refinement for SSA-1 obtained by Rietveld analysis. The tick marks (green) denote the peak positions of possible Bragg reflections.

In the Rietveld analysis, the background was fitted using a combination of Legendre polynomial function with 11 coefficients and a prior background profile determined by spline interpolation. A split pseudo-Voigt function of Toraya with an asymmetry correction was used to model the profile shape. Partial profile relaxation with a modified split pseudo-Voigt function was applied in a low  $2\theta$  angle region, which significantly improved fits against strong asymmetric and/or anisotropic broadened profiles. The  $\mu r$  ( $\mu$ : linear absorption coefficient,  $r$ : sample radius) values of the sample tubes was small (ca. 0.455 for SSA-1 and 0.398 for PML-1), then there was no need to correct for X-ray absorption. During the early stage of refinement, we imposed restraints upon all of the Si–O bond lengths and all the O–Si–O bond angles. Furthermore, restraints were imposed upon all of the bond lengths and bond angles, which were based on the molecular geometry of TEA<sup>+</sup> cation, during structural refinement. Obtained structural models were visualized by using the program VESTA3.

In the final refinement, the coordinates of 10 silicon sites, 22 oxygen sites, 8 carbon sites,

20 proton sites and 1 nitrogen site were refined, and virtual atom species were adapted to four terminal silanol oxygen atoms and OH<sup>-</sup> anion of TEAOH, whose H/O ratios was fixed to be one. Since these proton positions are usually disordered owing to highly motion, it is difficult to determine its position uniquely. However, scattering amplitude of proton was taken into account for the analysis. All of the isotropic atomic displacement parameters,  $B$ , for the Si sites were constrained to be equal:  $B(\text{Si}1) = B(\text{Sin}; n = 2-10)$ . Similar approximations of  $B(\text{O}1) = B(\text{On}; n = 2-22)$  and  $B(\text{Cn}; n = 1-8) = B(\text{N}1) = B(\text{OH}) = B(\text{Hn}; n = 1-20)$  were also imposed on the  $B$  parameters of the O sites and the C, N, and H sites, respectively, for convenience. Figure S3 shows difference plots obtained by the Rietveld analysis, indicating that our structural model is well agreement with observed data. Obtained  $R$  factors were sufficiently decreased to low levels, i.e.,  $R_{\text{wp}} = 5.7\%$  ( $S = 1.63$ ),  $R_F = 1.1\%$ , and  $R_{\text{Bragg}} = 1.6\%$ .

#### **4. Crystal structure analysis combined with DFT optimization of PML-1**

As mention in introduction, it was difficult to analyse the structure of PML-1 by means of PXRD data directly due to the lack of crystallinity. Furthermore, lattice constants were not determined uniquely by indexing analysis. So the most appropriate structure model of PML-1 was constructed by a combination of manually modelling, PXRD pattern simulation, and DFT optimization. Analysis procedure is shown below sequentially. (1) Lattice parameters ( $a$ ,  $b$ ,  $c$  and  $\beta$ ) of SSA-1 were gradually changed until peak positions of the experiment pattern of PML-1 coincided with the peak position calculated from lattice constants. Herewith, lattice constants of PML-1 were roughly determined as monoclinic symmetry. Subsequently, a PXRD pattern simulated from the constructed model was compared with experimental data in a  $2\theta$  range of 5–15°. Lattice parameters were optimized repeatedly. (2) Stacking period between adjacent silicate layer was analyzed. The fractional coordinates of framework atoms were moved along  $b$  direction until the simulated XRD pattern from constructed model is nearly consistent with experimental data in a  $2\theta$  range of 5–30°. (3) In this unit-cell, a crystal structure model, e.g., formation of Si–O–Si bridge in interlayer or modification of framework geometry, etc., was proposed by trial and error. (4) The

proposed model was further optimized by DFT calculation until total energy of the model is minimized. (5) The processes of (2), (3) and (4) were repeatedly conducted in regard to many proposed models, and the most appropriate model of PML-1 was obtained as shown in **Figure S4**.

Only by changing length of *b*-axis or *b* and *c*-axis, the simulated pattern of optimized model by DFT calculations was not consistent with experimental data of PML-1. This finding indicates that sliding between silicate layers occurred during calcination of SSA-1 disorderly, that is, conversion of PML-1 having disordered structure. Eventually, all lattice parameters and partial position of framework atoms had to be adjusted to make the simulated pattern agree with experimental data. Finally, the selected structure model of PML-1 was refined by the Rietveld method (**Figure S5**). In the refinement, geometrical constraints of  $l(\text{Si-O})$  and  $\phi(\text{O-Si-O})$  were always applied tightly, because low resolution data ( $d_{\text{min}} = 1.55 \text{ \AA}$ ) was used.

Four sites of H<sub>2</sub>O in micropore were found, however their occupancies,  $g(\text{WO})$ , could not be determined accurately. Therefore,  $g(\text{WO})$  values were constrained to be equal and was converged to 0.4. The presence of adsorbed water in micropore indicates hydrophilic property in spite of high silica composition and is strongly related with the internal silanols. In final refinement,  $g(\text{WO})$  was fixed at 0.4, and thermal displacement parameters,  $B$ , for all sites are constrained to be equal for conveniently. Additionally, thermal displacement parameters,  $B$ , for all sites are constrained to be equal. The number of adsorbed H<sub>2</sub>O was estimated to be 3.2 molecules per unit-cell, which can be calculated to be 0.047 g per 1 g of PML-1. This value is roughly estimated as 35 % of the maximum adsorption volume as shown in Fig. 8. Finally, Figure 12 shows the observed, calculated, and difference patterns for SSA-1 and PML-1 obtained by the Rietveld analysis, indicating that the structural model that we obtained explained the PXRD data well.

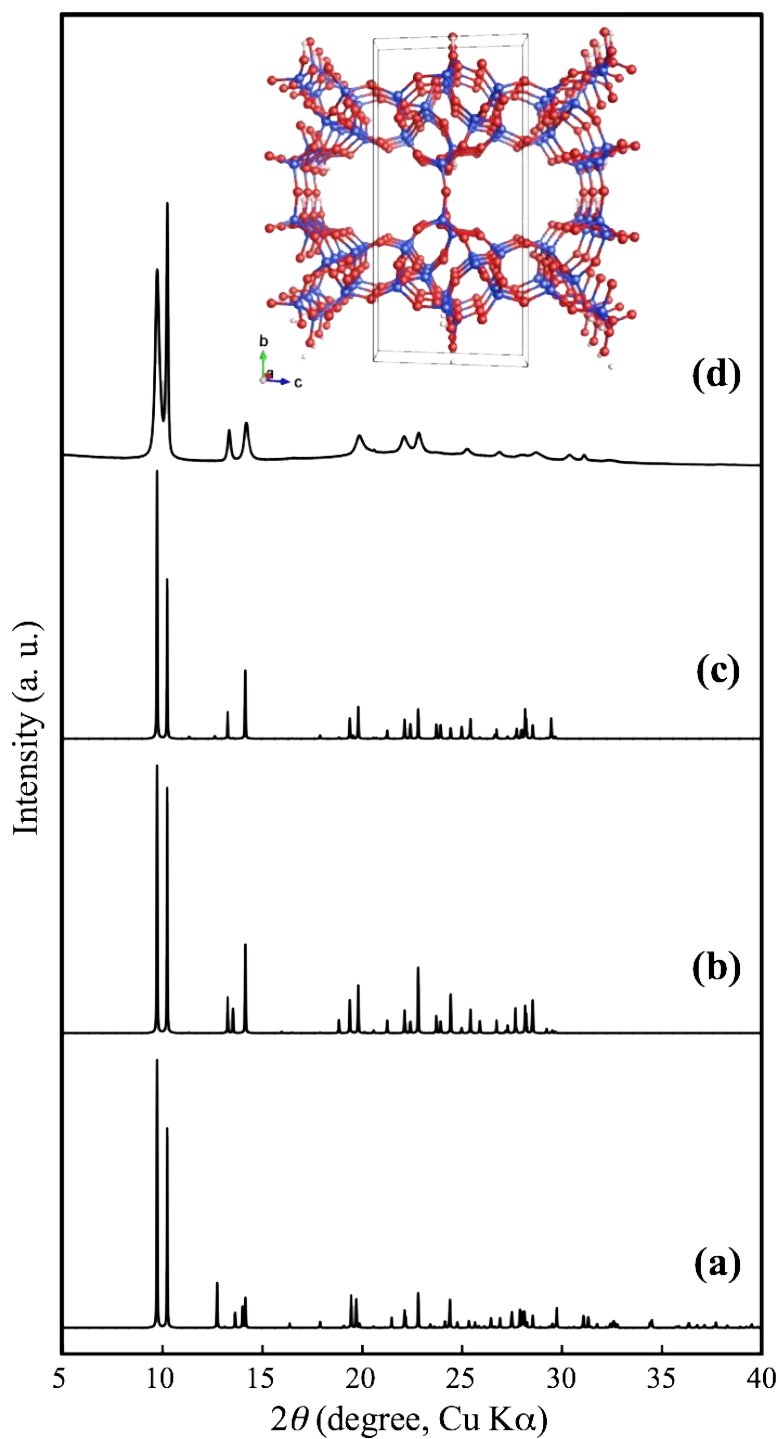


**Figure S4.** Simulated XRD patterns of models obtained by the DFT calculation: (a) *b* length changed model (b) *b* and *c* length changed model (c) the most appropriate model and (d) PML-1 (experimental). Inset figure indicates the most appropriate framework structural of PML-1 correspond to (c) viewed along [100] direction.



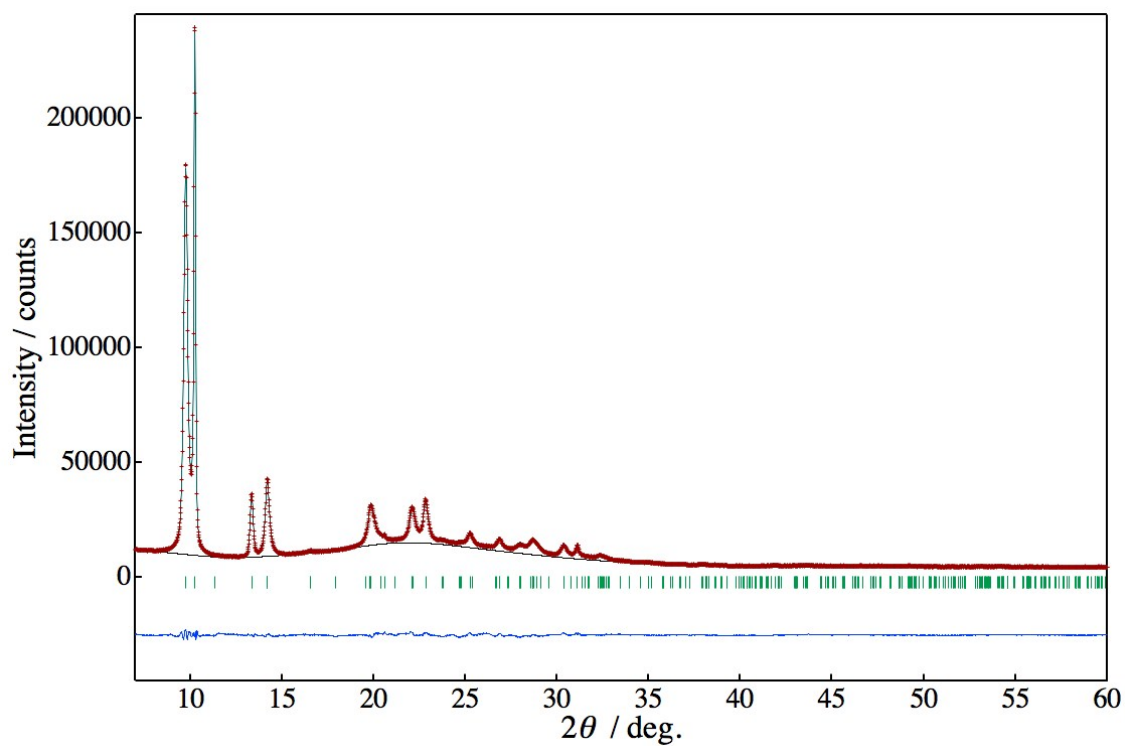


**Figure S5.** Observed pattern (red crosses), calculated pattern (light blue solid line), and difference pattern (blue) obtained by Rietveld refinement for PML-1 obtained by Rietveld analysis. The tick marks (green) denote the peak positions of possible Bragg reflections.

## 5. TG/DTA analysis of IEZ-SSA-1

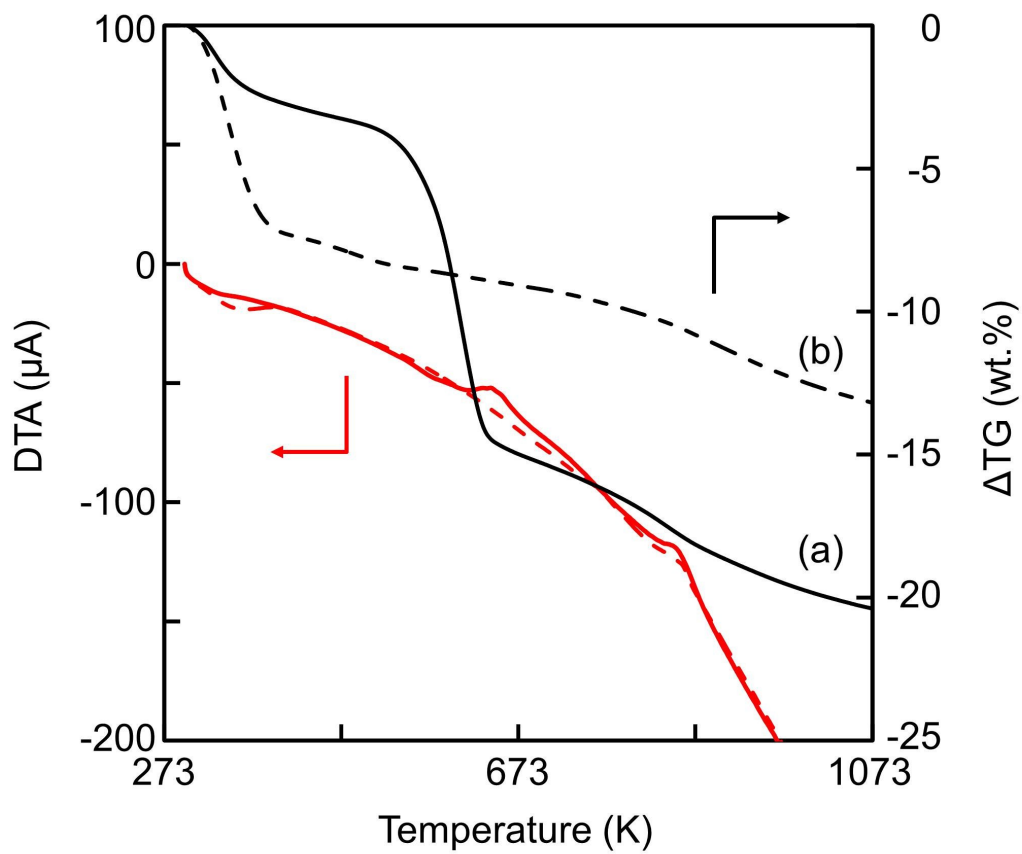


**Figure S6.** TG/DTA curves of (a) as-synthesized IEZ-SSA-1 (solid line) and (b) IEZ-SSA-1 (573 K) (dotted line).